Mine Water and the Environment (2019) 38:667–675
https://doi.org/10.1007/s10230-019-00621-5

TECHNICAL ARTICLE

Numerical Simulation and Risk Assessment of Water Inrush in a Fault Zone that Contains a Soft Infill

Zhuo Zheng[1] · **Rentai Liu**[1] · **Qingsong Zhang**[1]

Received: 29 July 2017 / Accepted: 31 July 2019 / Published online: 8 August 2019

Abstract
A numerical model was established to simulate the activation of the fault zone with a soft infill during a water inrush event. Distribution of the failed areas at different times was acquired. Then, a parametric sweep analysis was conducted to see the influence of permeability. By analyzing the results, a new parameter called the "activation coefficient" was proposed to characterize the fault zone activation process. A functional relationship was established between the activation coefficient and permeability. A series of numerical cases with different conditions were calculated to determine the parameters in the function. A method to evaluate the risk of water inrush is proposed, based on these results. By comparing the acceptable and actual values of the activation coefficient, the activation speed of the fault zone, and time for excavation and support can be determined; thus, the risk of water inrush can be evaluated. The research results were used during construction of line 1 of the Qingdao subway tunnel engineering project in China, which provided valuable data for assessing the risk of water inrush in a mine.

Keywords Water inrush mechanism · Fluid–solid interaction · Evaluation method · Finite element analysis

Introduction

Water inrush events are one of the most severe engineering disasters that can occur during mining and tunnel construction (Li et al. 2015a, b, c). It can occur suddenly and often at high pressure (Donnelly 2006; Zhang et al. 2009; Zuo et al. 2009). The consequence is usually destructive, causing severe casualty and property losses.

A fault zone may act as both an aquifer and an aquiclude, depending on the geological conditions and the influence of excavation. Groundwater elevation, pressure head, and flow direction may all be very heterogeneous within a fault zone. The heterogeneity of fault zones is mainly caused by its composition, which can consist of randomly occurring units of unaltered stiff rock fragments, surrounded by a soft, weak matrix. The matrix may be cemented by secondary minerals, which can easily lose its strength under the influence of groundwater. These geological masses can have a high risk of water inrush and require special consideration.

✉ Zhuo Zheng
413708318@qq.com

[1] Research Center of Geotechnical and Structural Engineering, Shandong University, Jinan 250061, China

A number of analytical models have been proposed to estimate the water inrush risk, such as the water inrush index, floor strata three zones, plate, and key strata models (Xiao et al. 1991; Miao et al. 2011; Shi and Singh 2001; Wang and Park 2003; Zhang 2005). On the other hand, Ma and Zhang (2012) proposed a water inrush evaluation method based on the Dempster-Schafer (D-S) evidence theory and the back-propagation (BP) neural network, which provides a useful tool for risk evaluation, except for some limitations of unstable output with certain deviations. Li and his groups (2011, 2012, 2013a, b) conducted a series of studies on water inrush evaluation methods.

In addition, a number of numerical simulations have been carried out to better understand the water inrush mechanism. Guo et al. (2009) proposed a method based on finite element theory to evaluate flow changes during water inrush events. Lu and Wang (2015) established a numerical model to calculate the process of fracture propagation under the influence of high pressure groundwater. Wu et al. (2011) proposed a water inrush simulation method that considers flow-solid coupling behavior and lagging effects.

However, the applicability of water inrush risk evaluation methodology is still limited, due to the complicated interaction between groundwater and rock mass. Moreover, the

effects of time should be sufficiently considered during engineering construction when a failure criterion is proposed. The risk of water inrush should be evaluated based on the activation speed of the fault zone and the available time for excavation and support. With these considerations, we established a numerical model to simulate fault zone activation during the water inrush process. The medium in the fault zone, including the failed area, is treated as a continuum, in which the stresses and strains are averaged over a representative volume. The failed area is characterized by changing the physical and mechanical properties of the elements whose stress state meet the failure criteria. Both the fluid flow and mechanical properties of the rock mass are considered in the fault zone activation process.

Numerical Experiment

General

For a rock mass with high integrity, the physical and mechanical properties are usually stable. In contrast, the physical and mechanical properties of a fault zone's infill materials are significantly influenced by surrounding conditions, such as crustal stress and groundwater. The permeability and mechanical characteristics can change greatly due to rock-water reactions or hydro-fracturing. The failure of soft media begins in local areas and gradually expands. When the failures accumulate to a threshold value, the whole geological mass may become unstable, leading to water inrush and other geological disasters.

The fundamental mechanisms of media-groundwater interactions must be studied to estimate the stability of soft infill media. The mechanical processes that must be considered are generally tensile or shear failure, or a combination of the two. Failure can be regarded as the total loss of integrity, or the formation of a yield area with a strain-softening response.

Fluid Behavior

The process of groundwater flow in the medium can be described by Darcy's law. The flow is driven by gradients in the hydraulic potential field of groundwater. According to Darcy's law, the net flux across a face of a porous control volume is expressed as:

$$u = -\frac{K}{\mu}(\nabla p + \rho g \nabla D) \tag{1}$$

Here, u is the Darcy's velocity of groundwater, ρ is the density of groundwater, p is fluid pressure, K is permeability of the medium, μ is fluid viscosity, g is gravitational acceleration, and D is the vertical coordinate. The continuity equation for the fluid is expressed as:

$$\frac{\partial}{\partial t}(\rho\phi) + \nabla \cdot (\rho u) = Q_m \tag{2}$$

where ϕ is the porosity, and Q_m is a mass source term. Porosity is defined as the fraction of the control volume that is occupied by pores. The storage coefficient S is defined as a weighted compressibility of the bulk aquifer material and the fluid in the pores. The relationship between the storage coefficient and porosity is expressed as:

$$\frac{\partial}{\partial t}(\rho\phi) = \rho S \frac{\partial p}{\partial t} \tag{3}$$

Inserting Eq. (1) and Eq. (3) into Eq. (2) produces the generalized governing equation:

$$\rho S \frac{\partial p}{\partial t} + \nabla \cdot \rho \left[-\frac{K}{\mu}(\nabla p + \rho g \nabla D) \right] = Q_m \tag{4}$$

Fracturing Process

The discrete-fracture and smeared-fracture methods are two approaches that have been used extensively to simulate hydraulic fractures. The discrete approach can precisely represent the physical nature of a crack, but it has some computational disadvantages (Bazˇant and Oh 1983; Suidan and Schnobrich 1973). The smeared-fracture method cannot precisely specify the boundary of the fracture, but it enables the simulation of fracture branching, fracture rotation, and multiple shear and tensile fractures in any direction without predetermination on fracture shape and location (Klerck 2000). In this study, the smeared-fracture approach was used to characterize the fracture process. The media, including the fractured and unfractured areas, is treated as a continuum, and the stresses and strains in the interior of the fracture are averaged over a certain representative volume.

The permeability of the infill medium alters when local failure occurs due to hydro-fracturing. The relationship between permeability and other parameters, such as porosity and volumetric strain, has been extensively investigated. According to Touhidi-Baghini (1998), permeability can be expressed as a function of the initial state of permeability, porosity, and volumetric strain:

$$\ln \frac{K}{K_0} = \frac{B}{\phi_0}\varepsilon_v \tag{5}$$

where K_0 and ϕ_0 are initial permeability and porosity, ε_v is the volumetric strain, and B is an empirical coefficient, and is set to 2 in the following calculation, based on the results of Touhidi-Baghini's study.

In the smeared-fracture method, the fracturing process is characterized by altering the physical and mechanical

properties of the mesh elements. Generally, the deformation modulus decreases due to the mechanical and chemical influence of groundwater. This process can be described by multiplying the initial modulus with a reduction factor. It should be noted that the mechanical behavior of the material is complicated since it is influenced by different stress conditions and loading paths, and was simplified in this study. The reduction factor was set to 0.1 when ε_v exceeds 0.2, which is a rough estimation for the calculation.

After the medium fails due to hydro-fracturing, the cementation between the grains is assumed to be totally broken, causing the medium to lose most of its strength. For a volumetric strain of 0.2, the deformation of the medium is quite large, which means that groundwater already flows in the voids between the grains, enhancing the decomposition of the medium. Thus, the reduction in this calculation is considered as a conservative value.

Solid Deformation

The stress–strain relationship of the medium with the influence of fluid pressure is expressed as:

$$\sigma = C \cdot \varepsilon - \alpha_B \cdot p \tag{6}$$

Here, σ is the Cauchy stress tensor, ε is the strain tensor, α_B is the Biot-Willis coefficient, p is the fluid pressure, and C is the elasticity matrix. According to Biot's theory, the storage coefficient can be expressed as a function of a combination of the Biot-Willis coefficient and the medium parameters:

$$S = \frac{\varepsilon}{K_f} + (\alpha_B - \varepsilon)\frac{1 - \alpha_B}{K_d} \tag{7}$$

Here, K_f is the fluid bulk modulus, K_d is the solid modulus. In this proposed model, the fluid flow and the deformation of the medium is coupled and solved numerically with the finite element method.

As the fracture medium is composed by many kinds of mineral particles with different cementation forms, the deformation modulus of the medium is heterogeneous. This characteristic can be described by a probability distribution function; the most widely used one is Weibull distribution shown in Eq. (8) (Weibull 1951), which characterizes the mechanical heterogeneity in various geo-materials and has been extensively studied by many researchers (Fang and Harrison 2002; Lu et al. 2013). Here, x represents any mechanical parameter of the solid medium; $\bar{x}$ represents the mean value of the mechanical parameter; λ is a distribution parameter, which represents the heterogeneity of the mechanical property of the medium. A range from 1 to 5 can basically cover most mechanical properties of geotechnical materials from highly homogeneous to highly heterogeneous. As λ increases, x is more narrowly constrained; thus, the mechanical property is more homogeneous. As λ decreases, x is distributed over a wider range, and the heterogeneous characteristic of the mechanical property increases (Fig. 1). In the following section, a value of 3 was used in the numerical calculation, which is a common value for geomechanical parameters (Lu et al. 2013).

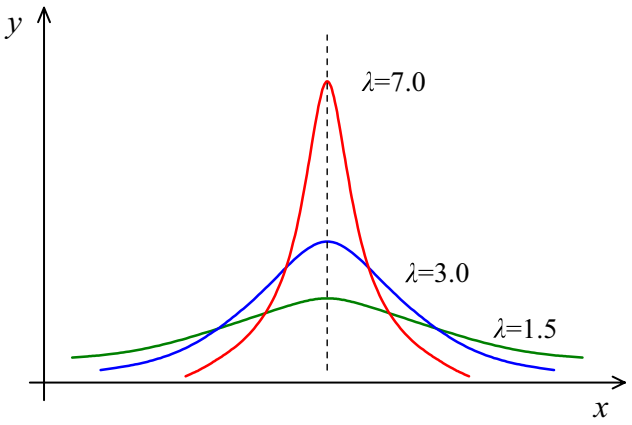

Fig. 1 Weibull distribution with different parameters

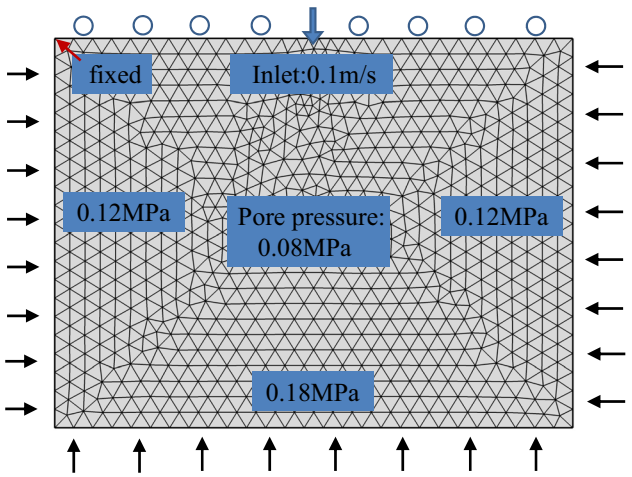

Fig. 2 Numerical model and boundary conditions

$$f(x, \bar{x}, \lambda) = \frac{\lambda}{\bar{x}} \cdot \left(\frac{x}{\bar{x}}\right)^{\lambda - 1} \cdot \exp\left[-\left(\frac{x}{\bar{x}}\right)^{\lambda}\right] \tag{8}$$

Numerical Model Set Up

A numerical model was established based on the theories mentioned above to study the mechanism of water inrush in a fractured zone (Fig. 2). The geometry of the studied

area was set to a rectangle with a height of 7.5 m and a width of 10 m. A normal load of 0.12 MPa was applied on the left and right side of the domain, and a normal load of 0.18 MPa was applied at the bottom, mimicking the crustal stress environment. The upper side of the domain is constrained with a displacement boundary condition: displacement in the vertical direction is set to zero, and the left endpoint is fixed as a reference point. An inlet with a length of 0.2 m was created in the middle of the top side. An inflow water flow velocity of 0.1 m/s was applied directly at the inlet to mimic a severely defected area of the fractured zone. A tentative calculation was carried out previously in order to see the corresponding pressure at the inlet. The result showed that the average pressure was ≈ 1.2 MPa. Thus, the water-head was assumed to be 120 m. The initial pore pressure was set at 0.08 MPa in the interior of the medium, considering a possible relatively impermeable initial surrounding condition. The water pressure on the left and right side was also 0.08 MPa. However, the water pressure on the bottom was set to zero, as the tunnel has been excavated and the fault zone revealed. The calculation parameters used in the numerical model are listed in Table 1.

Calculation Results and Analysis

The failure patterns of the medium under the influence of ground water at different times are shown in Fig. 3. The failed area appears first at the inlet and then gradually extends further. The pattern of the failed area resembles narrow channels. The failure in the medium is mainly due to hydro-fracturing, as water pressure acts on the solid medium and splits it at the front of the failed area, and impels the channel to propagate continuously. Initially, the water pressure acts normally on the solid medium. However, the channel extends at an inclined angle to the normal direction. This is probably because the solid medium bears a shearing failure. Afterwards, new failure tips appear along the channel wall and form new channels. The channels may start randomly at any weak point; thus, more than one channel may form. Then, these channels extend downward with nearly no

Table 1 Calculation parameters in the numerical model

Initial permeability	K_0	M^2	5.5×10^{-12}	Fluid viscosity	μ	Pa·s	0.001
Initial porosity	ϕ_0	–	0.45	Fluid compressibility	f	Pa^{-1}	4.5×10^{-10}
Maximum elastic modulus	E_{max}	MPa	12	Fluid density	ρ	kg/m^3	1000
Minimum elastic modulus	E_{min}	MPa	1.2	Biot-willis coefficient	α_B	–	1
Poisson's ratio	v	–	0.25	Inlet velocity	v_0	m/s	0.1

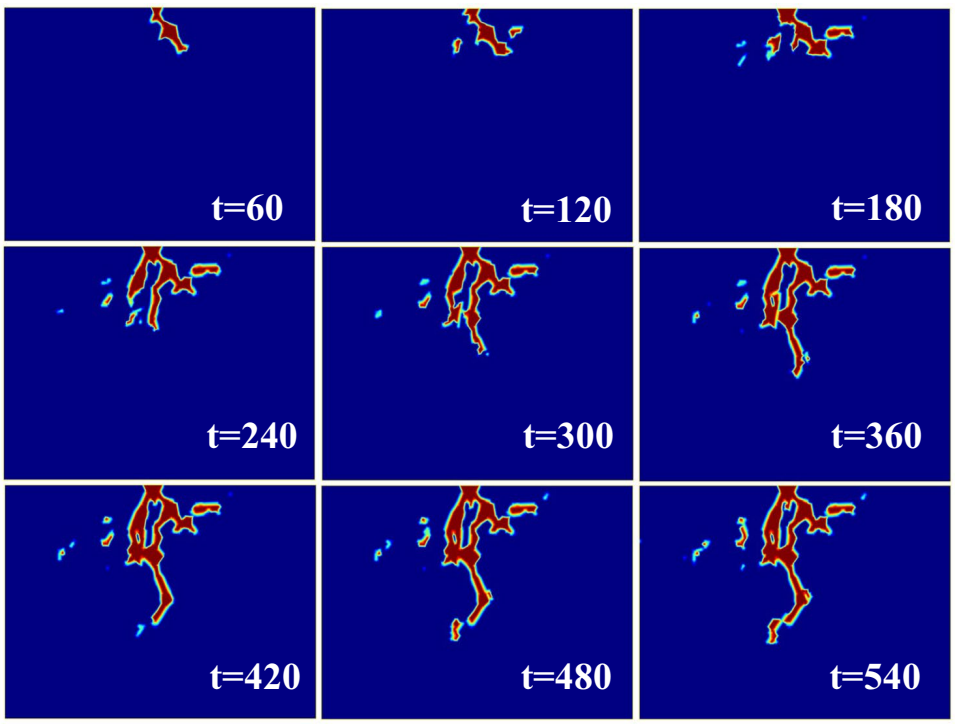

Fig. 3 Distribution of failed area at different times (sec)

inclined angle. At 540 s, more than two-thirds of the thickness of the medium had failed, and the convergence rate had significantly decreased during the simulation, since a systemic failure may occur in the medium. Thus, this stage may be assumed as a threshold for water-inrush.

Figure 4 shows the variation of the failed area and pressure at the inlet at different times. The failed area keeps increasing over time in an almost linear pattern. The water pressure at the inlet was calculated by averaging the pressure at every point along the inlet line. The actual pressure variation is characterized by the blue full line. Initially, the pressure increases from zero to a very high value (≈1.45 MPa) very quickly. Then it fluctuates a little until it deceases to almost 1.2 MPa. This process takes no more than 40 s. By referring to Fig. 3, it is obvious that the failed area that formed during this process was neglected. Thus, this fluctuation can be regarded as numerical instability during the initiation of the numerical calculation and was removed in the dashed line for approximation. With approximation, it is reasonable to assume that the pressure rises gradually in a time period between 0 and 200 s. During this period, a failed area in the shape of an inclined channel forms (Fig. 3). Next, the pressure deceases sharply from 1.45 MPa to almost 1.2 MPa. This process corresponds to the generation of several vertical channels (Fig. 3).

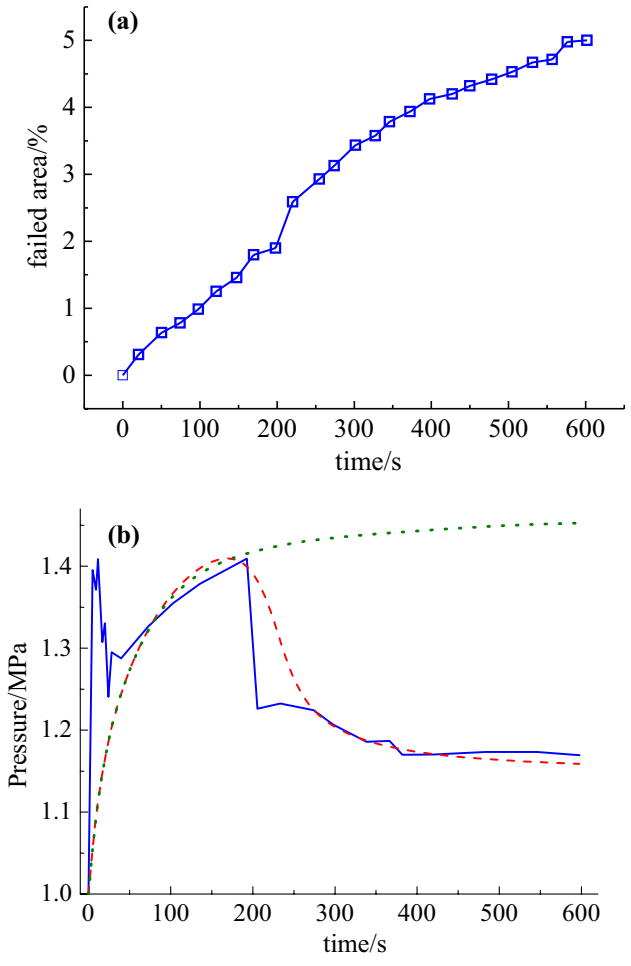

Fig. 4 **a** Relationship between time and failed area. **b** Relationship between time and water pressure at the inlet

The pressure drop means the resistance of the medium is less than it was initially. As the failed area in the medium accumulates, more weak areas are likely to be connected, so the risk of an inrush increases. The pressure variation is shown as a red dashed line. The trend increases at first, and then decreases. Since the boundary condition at the inlet is a flow rate controlled condition, it is reasonable to accept the pressure drop as the failed area increases. However, during the actual failure process that creates the fractured zone, the water pressure acting on the fracture's infill is unlikely to decrease. In fact, it may increase as the connectivity of the fracture grows. The actual trend of pressure variation is closer to the green dashed line, so the failure process of the medium is more likely to accelerate with time. Thus, the peak value of the red dashed line at 200 s may be assumed to be a threshold, after which the medium fails in an accelerating mode.

A parametric sweep was carried out for this calculation to see the influence of permeability changes on the failure patterns (Fig. 5). Initially, the growth of the failure area was somewhat similar. The inclined angle of the fracture channels were almost the same, except that the channel in the higher permeability medium was thicker. Afterwards, the failure patterns differed significantly. The failure area grows faster in the medium with higher permeability, and more fracture channels are likely to form. A comparison between the three columns shows that the permeability determines not only the length of the fracture channel, but also the formation of new channels. Since the permeability in the left panels of Fig. 5 is greater, it is easier for the first inclined channel to propagate further. The channel propagation has a higher resistance in the middle column, so the first channel ceases propagating after the new channel forms. For the right column, the permeability is so small that the failed area is constrained close to the inlet, which means that the risk of failure propagation is very small.

The corresponding accumulation curves are shown in Fig. 6. In the medium with a permeability of 9×10^{-12} m^2), the failed area was almost twice as large as in the medium with a permeability of 5×10^{-12} m^2, and six times larger than in the medium with a permeability of 1×10^{-12} m^2. For the first and second cases, the failed areas obviously keep increasing, so the risk of an inrush is very high. For the third case, the increment is very slow and it is more likely to reach a stable case, lowering the risk.

The sudden change shown in Fig. 4 does not occur in the two other cases. In the first case, the permeability of the medium is much greater, and the difference in

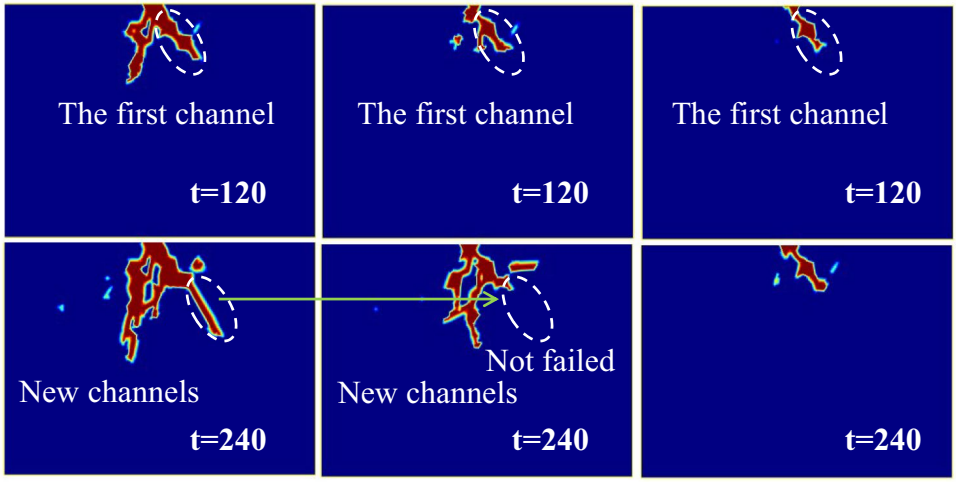

Fig. 5 Distribution of failed area in the medium with different permeability (permeability of the medium is 9×10^{-12} m^2, 5×10^{-12} m^2, and 1×10^{-12} m^2 for the left, middle, and right columns)

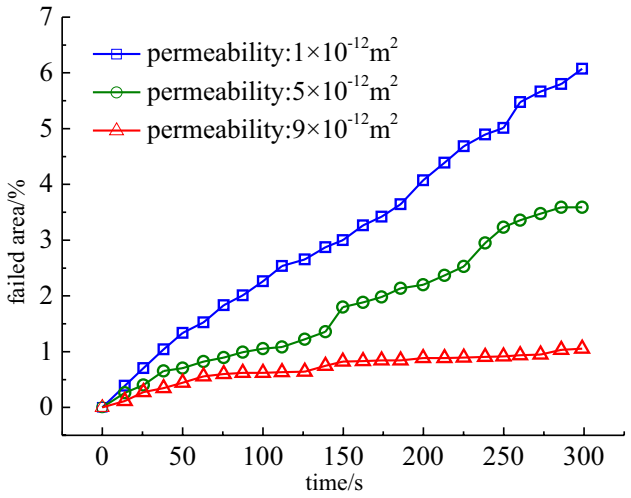

Fig. 6 Accumulation of failed area at different times (permeability of the medium is 9×10^{-12}, 5×10^{-12}, and 1×10^{-12} for the red, green, and blue lines)

resistance during hydro-fracturing of the channels was not so large. It can also be seen that the time interval between the development of the first channel and the new channels is very short. As shown in the left column in Fig. 5, the channels developed within 120 s. In fact, there is still a sudden pressure change in the failed area when the weak areas are connected, but this variation is not obvious. In the third case, the first channel was not sufficiently developed when the calculation ended, and the weak areas did not connect. Thus, no sudden change occurs. In sum, as the hydro-fracturing process develops, weak areas are likely to connect. If the difference in resistance is large enough, sudden changes will occur. Thus, the sudden change shown in Fig. 4 may be regarded as a fundamental mechanism of water inrush.

A New Criterion for Water Inrush Assessment

In order to analyze the speed of the activation process and the propagation of the failed area, a series of definition equations are proposed in this study: t_0 is called characteristic time, $\bar{t}$ is called dimensionless time, h is the height of the medium, and α is the percentage of the failed area to the fault fractured zone. The characteristic time is defined as the height of the medium divided by the water velocity at the inlet, and a dimensionless time is defined as the real time divided by the characteristic time.

$$t_0 = h/v_0 \tag{9}$$

$$\bar{t} = t/t_0 \tag{10}$$

A linear regression analysis was made between $\bar{t}$ and α, and the curve was forced through zero. A new parameter,β, called the activation coefficient, is proposed, defined as the slope of the regression line, which represents the speed of the activation process of the fractured zone.

$$\beta = \alpha/\bar{t} \tag{11}$$

A parameterized sensitivity analysis was conducted to see the influence of the medium permeability on β and the result is plotted on a linear-log graph (Fig. 7). The overall increasing trend shows some fluctuation; this may be due to the heterogeneity of the medium and the randomness of the propagation of the failed area. As permeability increases, the activation coefficient increases nonlinearly. The activation coefficient is very low when the permeability is less than 0.1, but the increasing rate suddenly changes afterwards. Then the activation coefficient keeps growing. When the permeability approaches 1, the increasing rate of β seems to slow down, and even deceases when the permeability changes from 0.8 to 0.9. This may be because the influence of the heterogeneity of the medium exceeds that of the

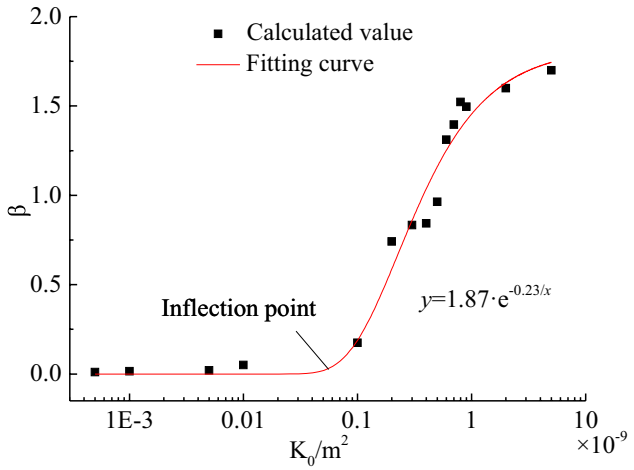

Fig. 7 Relationship between activation coefficient and permeability

initial permeability. When the permeability exceeds 1, the rate changes very little.

A fitting analysis was carried out to characterize the relationship between permeability and the activation coefficient according to the calculated results. The fitting function is established based on the following assumptions: First, the activation coefficient, β, should approach zero when the permeability is infinitely small, since an activation process cannot develop in an impermeable layer. Thus, the function is forced through zero. Second, there should be an upper limit of β when the permeability is very high, as the speed of the activation process cannot be infinitely high for a specific condition of the medium.

On this basis, an exponential type function was chosen for the fitting, as shown in Eq. (12). Since these two variables are positively correlated, there is a negative sign before parameter b. The curve is forced through zero and has a horizontal asymptotic line, according to the above assumptions. When x approaches infinity, y approaches a, thus representing the upper limit of the activation process, which is influenced by the rock mass properties and the water pressure. The value of b influences the form of the curve. The curve becomes steeper and converges more rapidly when b is smaller. Thus, b characterizes the difficulty of the activation process.

$$y = a \cdot e^{-b/x} \tag{12}$$

It can be seen from Fig. 7 that β increases slowly with K_0 at the beginning of the curve and that there is an inflection point after which the rate obviously becomes greater. That means that there may be a critical point before which the activation process may not happen quickly. This critical point is mainly determined by b, since this parameter largely controls the pattern of the curve. The value of b is mainly influenced by the uniformity of the medium. When the medium is highly non-uniform, it contains more weak areas, even when the overall mechanical strength and the impermeability are high. These areas provide more opportunities for the groundwater to break though the medium. Thus, for a calculation value before the critical point, excavation through the fault-fractured zone is feasible as long as care has been taken, such as by reinforcement of the formation by pre-grouting and in-time lining.

The relationship between the permeability and activation coefficient may change for different conditions, such as the strength of the medium and the crustal stress. However, these factors may only make a limited difference to the value of a and b, and the overall functional form may not change. To determine the value of the parameters in the function, different conditions were considered in the numerical model. The value of a was set to 1.87, as obtained in the fitting analysis (Fig. 8). The influence of crustal stress and modules of the medium on parameter b was numerically analyzed (Table 2). The modulus was varied from 1 to 50 MPa, and the crustal stress was varied from 0.05 to 0.25 MPa. Thus, by using the results in Table 2, the value of b can be determined by interpolation or extrapolation.

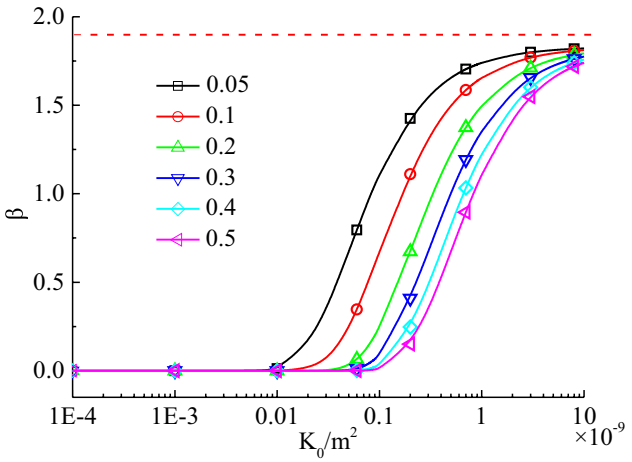

Fig. 8 The functional curve with different values of parameter b ($a = 1.87$)

Table 2 Determination on b according to calculation results with different modulus and crustal stress ($a = 1.87$)

Crustal stress (MPa)	Modulus				
	1 MPa	5 MPa	10 MPa	20 MPa	50 MPa
0.05	0.07	0.11	0.15	0.22	0.28
0.10	0.11	0.17	0.20	0.27	0.33
0.15	0.17	0.23	0.28	0.31	0.38
0.20	0.22	0.25	0.32	0.36	0.42
0.25	0.27	0.32	0.35	0.42	0.48

It should be noted that the proposed criterion is mainly based on the calculated results of this numerical model, which was used to investigate the relationship between the activation degree of the fault and its mechanical and hydraulic properties, such as its deformation modulus and permeability. In practical engineering, it can be difficult to acquire complete information on the fault-fractured zone, and the mechanism of water inrush is complex. As the criterion is mainly based on numerical simulation, the validity and applicability still had to be further investigated.

Engineering Application

The risk evaluation method was used during construction of line 1 of the Qingdao subway tunnel in China. The subway line goes under the Jiaozhou Bay of the Huanghai Sea. The length of the tunnel in this area is 3.45 km. According to geological exploration, seven fault zones were located along the tunneling direction. The rock mass in the fault zones were III and IV grade, according to The Standard for Engineering Classification of Rock Mass (GB50218—94, The National Standards Compilation Group of People's Republic of China 1995), which is not stable under the influence of groundwater. During excavation, the permeability, crustal stress, and modulus of the medium were measured for each of the faults and the estimated activation coefficient was calculated using Eq. (12) and Table 2. Then, the acceptable value of the activation coefficient was calculated using Eqs. (9)–(11).

Determining the value of v_0 is difficult, as it cannot be directly measured before excavation. Thus, alternatives should be adopted to approximate it. Here, the value of v_0 was approximated as the predicted inflow of water into the tunnel using the tunnel inflow prediction methods proposed by Hwang and Lu (2007) and Kolymbas and Wagner (2007). The height of the medium was determined by geological exploration data, allowing the characteristic time to be determined. It should be noticed that these approximations reduce the accuracy of the water inrush risk evaluation, and should be used carefully. Other methods, such as the water inrush coefficient method, should also be used for a comprehensive evaluation on the water inrush risk.

Generally, excavation and construction of a tunnel section takes about 7–10 days, so this value was used as the real time. According to the analysis above, water inrush can occur after half of the medium fails, and thus the value of α is about 0.5. However, as water inrush can be induced by the failure of a small, but critical, portion of the rock mass, and the mechanical properties of the rock mass are quite different for different geotechnical engineering projects, this value should be reduced for security, depending on the geological conditions. An acceptable value for the activation coefficient can then be determined, as shown in Fig. 9. For most of the faults, the actual value was far less than the acceptable value; thus, the risk of water inrush was low. For the no. 6 fault, the actual and acceptable values were very close. Thus, grouting reinforcement was conducted during the excavation of this section. The water inflow amount was reduced remarkably and the activation coefficient decreased from 0.55 to 0.41, which minimized the risk of water inrush. However, the validity of this method still needs to be further evaluated and tested in different engineering projects.

Conclusions

We evaluated the risk of water inrush in a fault zone during subsea tunnel excavation using a numerical model based on continuum theory. The failed area was characterized by changing the physical and mechanical properties of the elements whose stress state meet the fracturing criteria. Both the flow and mechanical properties are included in this process. Results show that the proposed model can successfully simulate the activation of the fault zone.

Initially, the channel extends at an inclined angle to the normal direction because the solid medium bears a shearing failure. Afterwards, new failure tips appeared along the channel wall and new channels formed. The channels can starts randomly at any weak point, so multiple channels may form. The overall failed area keeps increasing with time in an almost linear pattern.

A new parameter, called the "activation coefficient" (β) is proposed based on the numerical results, which characterizes the speed of the fault zone activation process. A functional relationship was established between the activation coefficient and the permeability. A critical point exists

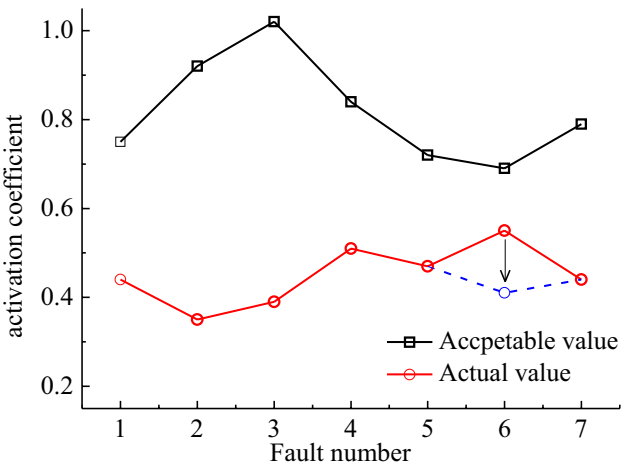

Fig. 9 Comparison between acceptable and actual values of the activation coefficient

before which the activation process may not happen in a short period of time, which means excavation through the fault-fractured zone is feasible as long as care has been taken, such as reinforcement of the formation by pre-grouting and, in time, lining.

The risk of water inrush can be evaluated by comparing the acceptable and actual values of the activation coefficient. Thus, the activation speed of the fault zone, excavation, and support time can be determined. However, it should be noted that the proposed criterion is mainly based on the results of this numerical model, and, in practice, it is difficult to acquire such information about a fault-fractured zone. To ensure safety, the risk of water inrush should be evaluated based on a variety of methods and comprehensive analysis.

Acknowledgements This work was financially supported by the General Program of the National Natural Science Foundation of China (51779133), National Key R&D Plan of China (2016YFC0801604), and Joint Funds of the National Natural Science Foundation of China (U1706223). The authors thank the editors and two anonymous reviewers for their careful work and thoughtful suggestions.

References

Bazˇant ZP, Oh BH (1983) Crack band theory for fracture of concrete. Mater Struct 16(3):155–177

Donnelly LJ (2006) A review of coal mining induced fault reactivation in Great Britain. Q J Eng Geol Hydrogeol 39(1):5–50

Fang Z, Harrison JP (2002) Development of a local degradation approach to the modelling of brittle fracture in heterogeneous rocks. Int J Rock Mech Min 39(4):443–457

Guo H, Adhikary D, Craig M (2009) Simulation of mine water inflow and gas emission during longwall mining. Rock Mech Rock Eng 42(1):25–51

Hwang JH, Lu CC (2007) A semi-analytical method for analyzing the tunnel water inflow. Tunn Undergr Space Technol 22(1):39–46

Klerck PA (2000) The finite element modeling of discrete fracture in quasi-brittle materials. PhD diss, University of Wales, Swansea

Kolymbas D, Wagner P (2007) Groundwater ingress to tunnels—the exact analytical solution. Tunn Undergr Space Technol 22(1):23–27

Li X, Li Y, Zhou S (2011) Study and application of forecasting system for water inrush under high pressure in Xiamen submarine tunnel construction based on GIS. Proc Environ Sci 10:999–1005

Li Z, Wang X, Xie L (2012) Risk evaluation and comprehensive geological prediction based on fuzzy wavelet neural network during tunneling in karst area. Electron J Geotech Eng 17:2155–2167

Li SC, Zhou ZQ, Li LP, Xu ZH, Zhang QQ, Shi SS (2013a) Risk assessment of water inrush in karst tunnels based on attribute synthetic evaluation system. Tunn Undergr Space Technol 38:50–58

Li SC, Zhou ZQ, Li LP, Shi SS, Xu ZH (2013b) Risk evaluation theory and method of water inrush in karst tunnels. Chin J Rock Mech Eng 32(9):1858–1867

Li LP, Zhou ZQ, Li SC, Xue YG, Xu ZH, Shi SS (2015a) An attribute synthetic evaluation system for risk assessment of floor water inrush in coal mines. Mine Water Environ 34:288–294

Li LP, Lei T, Li S, Zhang Q, Xu Z, Shi S, Zhou Z (2015b) Risk assessment of water inrush in karst tunnels and software development. Arab J Geosci 8(4):1843–1854

Li SC, Liu B, Nie L, Liu Z, Tian M, Wang S, Su X, Guo Q (2015c) Detecting and monitoring of water inrush in tunnels and coal mines using direct current resistivity method: a review. J Rock Mech Geotech Eng 7(4):469–478

Lu Y, Wang L (2015) Numerical simulation of mining-induced fracture evolution and water flow in coal seam floor above a confined aquifer. Comput Geotech 67:157–171

Lu YL, Elsworth D, Wang LG (2013) Microcrack-based coupled damage and flow modeling of fracturing evolution in permeable brittle rocks. Comput Geotech 49(4):226–244

Ma J, Zhang YM (2012) A new dynamic assessment for multi-parameters information of water inrush in coal mine. Proc Eng 26:759–764

Miao XX, Cui XM, Wang JA, Xu JL (2011) The height of fractured water-conducting zone in undermined rock strata. Eng Geol 20(1):32–39

Shi L, Singh RN (2001) Study of mine water inrush from floor strata through faults. Mine Water Environ 20(3):140–147

Suidan M, Schnobrich WC (1973) Finite element analysis of reinforced concrete. J Struct Div ASCE 99:2109–2122

The National Standards Compilation Group of People's Republic of China (1995) GB50218—94 Standard for engineering classification of rock mass. China Planning Press, Beijing **(in Chinese)**

Touhidi-Baghini A (1998) Absolute permeability of McMurray formation oil sands at low confining stresses. PhD diss, Univ of Alberta, Canada

Wang JA, Park H (2003) Coal mining above a confined aquifer. Int J Rock Mech Min 40(4):537–551

Weibull W (1951) A statistical distribution function of wide applicability. J Appl Mech 13(2):293–297

Wu Q, Zhu B, Liu SQ (2011) Flow-solid coupling simulation method analysis and time identification of lagging waterinrush near mine fault belt. Chin J Rock Mech Eng 30(1):93–104 **(in Chinese)**

Xiao GC, Irvin RA, Farmer IW (1991) Water inflows into longwall workings in the proximity of aquifer rocks. Min Eng 151(358):9–13

Zhang JC (2005) Investigations of water inrushes from aquifers under coal seams. Int J Rock Mech Min Sci 42:350–360

Zhang HQ, He YN, Tang CA, Ahmad B, Han LJ (2009) Application of an improved flow-stress-damage model to the critically assessment of water inrush in a mine: a case study. Rock Mech Rock Eng 41(6):911–930

Zuo JP, Peng SP, Li YJ, Chen ZH, Xie HP (2009) Investigation of karst collapse based on 3-D seismic technique and DDA method at Xieqiao coal mine. China. Int J Coal Geol 78(4):276–287